Drosophila chibby is required for basal body formation and ciliogenesis but not for Wg signaling

Camille Enjolras,[1] Joëlle Thomas,[1] Brigitte Chhin,[1] Elisabeth Cortier,[1] Jean-Luc Duteyrat,[1] Fabien Soulavie,[1] Maurice J. Kernan,[2,3] Anne Laurençon,[1] and Bénédicte Durand[1]

[1]Centre de Génétique et de Physiologie Moléculaire et Cellulaire, Centre National de la Recherche Scientifique UMR 5534, Université Claude Bernard Lyon 1, Villeurbanne, Lyon F69622, France
[2]Department of Neurobiology and Behavior and [3]Center for Developmental Genetics, Stony Brook University, Stony Brook, NY 11794

Centriole-to–basal body conversion, a complex process essential for ciliogenesis, involves the progressive addition of specific proteins to centrioles. CHIBBY (CBY) is a coiled-coil domain protein first described as interacting with β-catenin and involved in Wg-Int (WNT) signaling. We found that, in *Drosophila melanogaster*, CBY was exclusively expressed in cells that require functional basal bodies, i.e., sensory neurons and male germ cells. CBY was associated with the basal body transition zone (TZ) in these two cell types. Inactivation of *cby* led to defects in sensory transduction and in spermatogenesis. Loss of CBY resulted in altered ciliary trafficking into neuronal cilia, irregular deposition of proteins on spermatocyte basal bodies, and, consequently, distorted axonemal assembly. Importantly, *cby*[1/1] flies did not show Wingless signaling defects. Hence, CBY is essential for normal basal body structure and function in *Drosophila*, potentially through effects on the TZ. The function of CBY in WNT signaling in vertebrates has either been acquired during vertebrate evolution or lost in *Drosophila*.

Introduction

The structure and protein composition of cilia are highly conserved across eukaryotes. A cilium is built on a basal body derived from the mother centriole. Centriole maturation into a basal body is a complex process that includes the progressive addition of different protein structures including transition fibers, basal feet, and ciliary rootlets (Hoyer-Fender, 2010; Ishikawa and Marshall, 2011). The prototypical centriole found in most organisms is a radially symmetric arrangement of nine microtubule triplets. However, Ecdysozoa such as *Caenorhabditis elegans* and *Drosophila melanogaster* show major differences in the ultrastructure of centriole/basal bodies. In *C. elegans*, the centriole is composed of singlet microtubules, not triplets. In *Drosophila*, centrioles in embryos and most tissues are composed of microtubule doublets. In spermatocytes of the *Drosophila* male germ line, centrioles do show the prototypical nine triplets but lack some of the maturation structures found in other eukaryotes.

Ciliogenesis starts with the docking of the basal body, either directly to the membrane at the cell surface or to cytosolic vesicles that will eventually fuse to the plasma membrane (Sorokin, 1968). An initial extension of microtubule doublets from the basal body constitutes a specialized transition zone (TZ) delineated by specific localized proteins and by structures such as transition fibers, which link the basal body to the membrane and form a selective barrier to transport into the cilium (Ishikawa and Marshall, 2011). Further extension of the axoneme and ciliary membrane above the cell surface requires intraflagellar transport (IFT), in which specialized kinesin and dynein motors move an IFT protein complex and associated cargoes from the base to the tip of the cilium and back (Rosenbaum and Witman, 2002; Ishikawa and Marshall, 2011). Two notable exceptions to the IFT mode of assembly are the flagella of *Plasmodium* and of *Drosophila* sperm (Han et al., 2003; Sarpal et al., 2003; Briggs et al., 2004). *Drosophila* sperm axonemes are first fully extended in a cytoplasmic syncytium, independent of IFT, and only then ensheathed by a plasma

THE JOURNAL OF CELL BIOLOGY

The Rockefeller University Press $30.00
J. Cell Biol. Vol. 197 No. 2 313–325
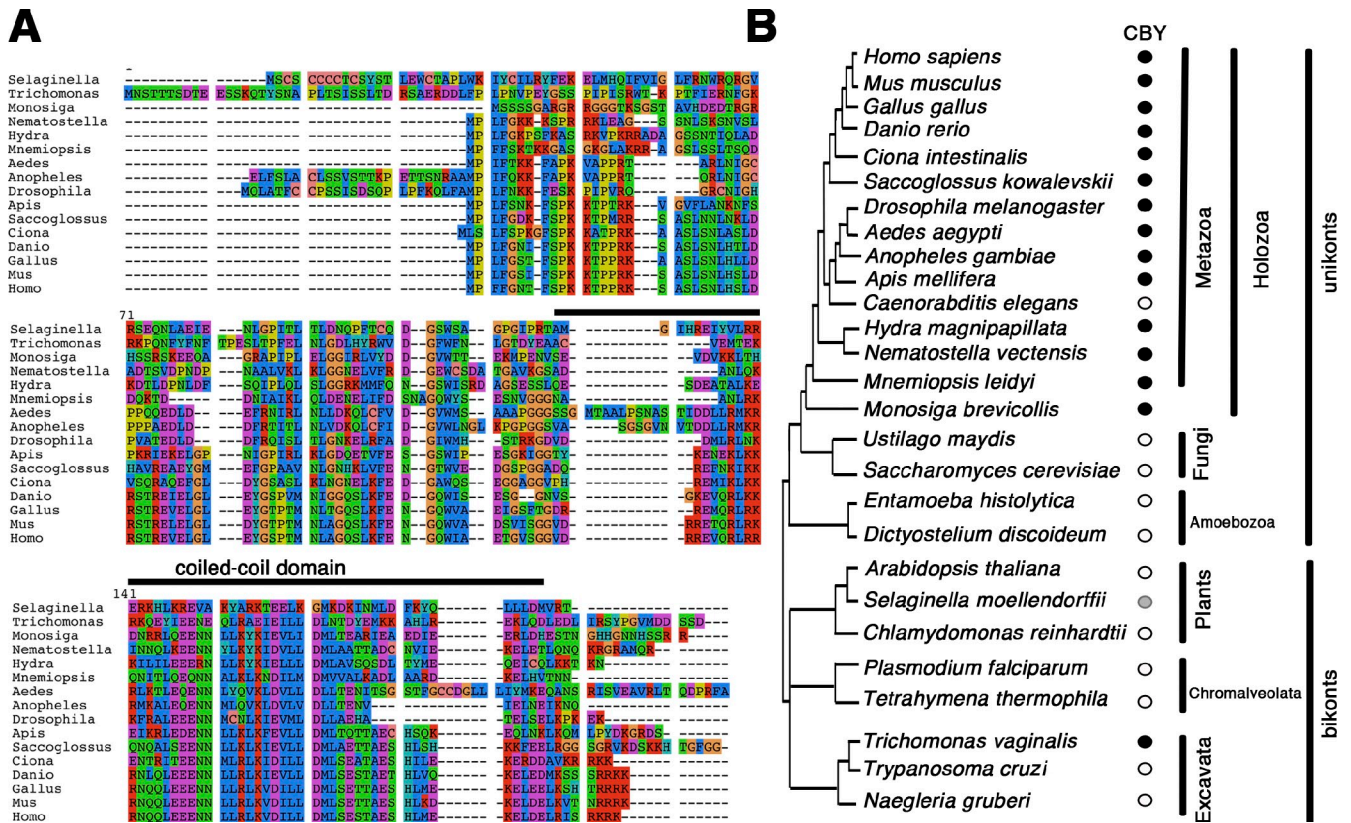www.jcb.org/cgi/doi/10.1083/jcb.201109148

JCB 313

Figure 1. CBY conservation in animals. (A) CBY is a small protein with a conserved coiled-coil domain close to the C terminus, highly conserved in animals (black bar). Each of the eight classes of amino acids is represented by one color. (B) Orthologs of CBY are found in animals with motile cilia (black filled circles) and in the closest unicellular relatives of animal, the marine choanoflagellate *Monosiga brevicollis*, but not in nematode genomes or in most unicellular organisms (open circles). A probable homolog is found in the parabasalid protist *Trichomonas*, and a more distant relative is found in the club moss *S. moellendorffii* (gray circle). CBY is not found in most bikonts (open circles).

membrane, during spermatid individualization (Fuller, 1993). However, a form of centriole maturation does occur earlier in *Drosophila* spermatogenesis: in primary spermatocytes, all four centrioles extend a distal zone formed of nine doublets and ensheathed by a membrane cap. The elongated centrioles migrate to the plasma membrane, where the distal segment protrudes from the cell surface and hence resembles a short cilium (Tates, 1971; Fuller, 1993). The function of this transient primary cilium is unknown. *unc* mutants, in which it is shortened, can proceed through an apparently normal meiosis (Baker et al., 2004). At the onset of meiosis I, the pairs of elongated centrioles are engulfed together with their membrane caps and relocalized to the meiotic spindle poles (Tates, 1971). These observations strongly suggest that basal body and TZ-like structures assemble in *Drosophila* spermatocytes before meiosis and flagellar elongation.

In vertebrates, cilia are required during development to mediate signal transduction pathways such as the sonic hedgehog pathway (Goetz and Anderson, 2010). Defects in cilia or cilia-associated proteins are also associated with defective Wg-Int (WNT) and planar cell polarity signaling, although some of the data are contradictory, and the precise mechanism is far from understood (Ajima and Hamada, 2011; Wallingford and Mitchell, 2011). To date, reports of an association between cilia and Wingless (Wg) signaling are limited to vertebrates,

with one notable exception: the CHIBBY (CBY) protein. CBY was first identified as an interactor with β-catenin in humans, and RNAi experiments targeting *cby* expression implied that CBY negatively regulates WNT signaling both in mammalian cell culture and in *Drosophila* (Takemaru et al., 2003). Identified as PIGEA-14, CBY was also shown to be associated with polycystin-2, a ciliary ion channel (Hidaka et al., 2004). Last, *cby*$^{-/-}$ mutant mice showed defective airway function associated with impaired basal body docking, reduced number of motile cilia (Voronina et al., 2009; Love et al., 2010), and increased expression of β-catenin regulatory targets (Love et al., 2010).

We have identified *Drosophila cby* as a putative target of the RFX transcription factor, which activates transcription of many genes required for the assembly of cilia (Dubruille et al., 2002; Laurençon et al., 2007). Together, these observations suggested a possible link between Wg signaling components and cilia in *Drosophila*. We show here that *Drosophila cby* is expressed only in cells that harbor cilia, namely in ciliated type I sensory neurons and in male germ cells. CBY protein is associated with the maturing basal bodies and TZ in these two cell types. *cby*-null mutant flies show sensory transduction defects and male hypofertility but no evidence of Wg signaling defects. We show that CBY is required in ciliated neurons for proper TZ and axonemal assembly and for protein trafficking into or
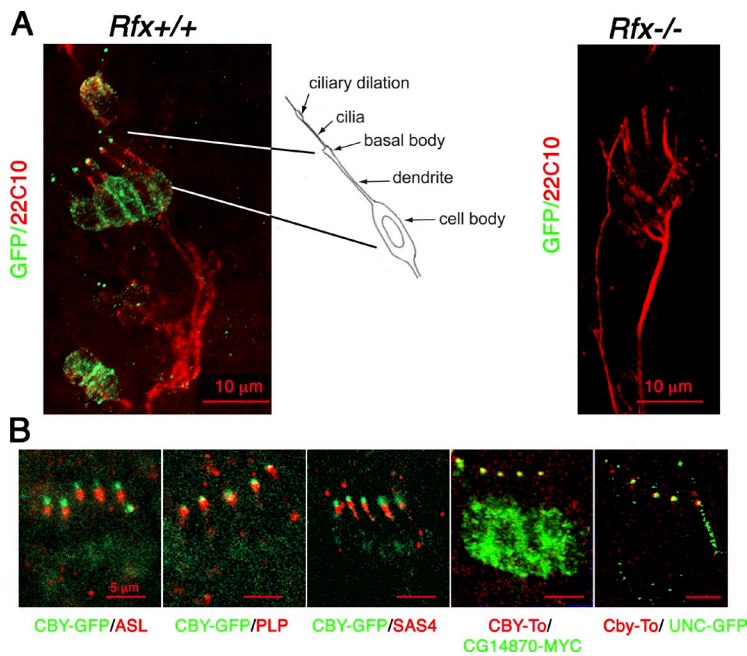
Figure 2. ***cby* is expressed in ciliated neurons of the *Drosophila* PNS.** (A) Transgenic flies expressing *cby* coding sequences fused to GFP under *cby* regulatory sequences were analyzed for GFP expression. GFP expression is detected only in type I ciliated cells of the PNS in *Rfx⁺/⁺* flies (left). GFP staining is observed in the cytosol and mainly as a dot at the tip of the dendrite. The PNS is labeled (red) with an anti-Futsch antibody (22C10). In *Rfx⁻/⁻* flies, the *cby* reporter construct is not expressed (right). (B) Double labeling of a transgenic fly strain expressing *cby* coding sequences fused to the fluorescent reporters GFP or Tomato under *cby* regulatory sequences with different markers of the centriole. CBY is localized at the tip of the centriole/basal body, as observed with ASL, PLP, SAS4, UNC fused to GFP, and CG14870 fused to a MYC epitope. CBY colocalizes with the TZ marker CG14870.

out of the cilia. In spermatogenesis, CBY is also required for centriole-to–basal body conversion, as revealed by defective basal body–associated uncoordinated (UNC) protein deposition. Last, we show that *cby* is required for axonemal assembly during spermiogenesis. Altogether our results imply that, in *Drosophila*, CBY functions in basal body/TZ biogenesis but not in WNT signaling.

Results

The RFX target gene *cby* is expressed in *Drosophila* ciliated cells, and CBY is associated with maturing basal bodies

CBY, a small protein with a C-terminal coiled-coil domain, is found in all ciliated unikont animals, with the exception of *C. elegans* and other nematodes (Fig. 1). CBY is also found in choanoflagellates, which can have a colonial life and are closely related to animals (King et al., 2008). Two probable CBY homologs are also present in the Excavate protist *Trichomonas vaginalis* and two possibly related proteins in the lower plant *Selaginella moellendorffii* (which has flagellated zoospores). Their occurrence suggests that a CBY homolog was present in the universal ancestral eukaryote. However, no CBY-related protein could be identified in any other bikont genomes, including well-studied ciliated organisms such as *Chlamydomonas reinhardtii*, *Trypanosoma*, or *Paramecium*. The Excavates have been proposed to stem from a very deep branching of the eukaryotic tree but with a closer association with bikonts than with unikonts (Hampl et al., 2009); the *Trichomonas cby* homolog instead favors a closer association with the unikonts.

Drosophila cby was identified in a screen for potential regulatory targets of the transcription factor RFX (Laurençon et al., 2007). To analyze *cby* expression in *Drosophila*, we constructed two transgenes including the *cby* promoter and entire coding sequence, fused at the C terminus to GFP or to Tomato (see Materials and methods). In transgenic embryos, expression of both constructs was restricted to type I sensory neurons of the peripheral nervous system (PNS), the only ciliated cells in the embryo. The fusion protein was found in the cell body and as a dot at the tip of the sensory process in all type I sensory neurons (Fig. 2 A). No expression was detectable in any other parts of the embryo (unpublished data). In an *Rfx* mutant background, *cby* expression was lost, confirming that in the PNS, *cby* is regulated by RFX (Fig. 2 A).

By coimmunolabeling with the centriole/basal body markers Asterless (ASL), pericentrin-like protein (PLP), and SAS-4, CBY was located more precisely at the tip of the basal body to a region that likely corresponds to the TZ between the basal body and the cilium proper (Fig. 2 B). To confirm this hypothesis, we looked at CBY location relative to B9D1/Meckel syndrome (MKS) 1–related (MKSR1), one of three interdependent B9 domain proteins involved in assembling the TZ (Bialas et al., 2009; Williams et al., 2011). Its *Drosophila* ortholog is encoded by CG14870 and is expressed in ciliated cells (Avidor-Reiss et al., 2004). We made a CG14870-MYC reporter construct, with the promoter and complete coding sequences fused to a MYC epitope, and found that CBY-Tomato and CG14870-MYC were indeed colocalized at the distal end of the basal body (Fig. 2 B). Hence, CBY is associated with the TZ of *Drosophila* sensory cilia. UNC, a basal body–associated protein required for axoneme structural integrity (Baker et al., 2004), also colocalized with CBY at the distal end of basal bodies in type I sensory neurons (Fig. 2 B).

cby was also expressed in larval and adult testis. CBY was associated with the duplicated elongating centrioles in G2 spermatocytes and with basal bodies in early spermatids (Fig. 3, A1–3 and 6–8). No *cby* expression was found associated with

Figure 3. ***cby* is expressed during spermatogenesis.**
(A) The diagram shows the cycle of the centriole during spermatogenesis. In G2 spermatocytes, the two pairs of replicated centrioles elongate and reach the membrane before meiosis entry, and single centrioles are distributed to each of the haploid spermatids after meiosis. (A1–3) CBY-GFP is localized at the tip of the elongating centrioles labeled for γ-tubulin (γTUB) from early G2 spermatocytes to early spermatids. (A4 and 5) As sperm axoneme elongates, CBY is found at the tip of the axoneme and lost from the basal body (white arrows). Note that some CBY-GFP is found associated with mitochondria during spermatid elongation (white arrowhead). (A6–10) CBY-TOMATO localization in live squashes of *Drosophila* testis expressing UNC-GFP. (A6–8) CBY is localized at the tip of the elongating centriole adjacent to the UNC-GFP staining from spermatocytes to early spermatid stage. CBY-TOMATO is transiently associated with the mitochondria (arrowhead). (A9 and 10) In elongating spermatids, CBY-TOMATO is associated with UNC-GFP only at the tip of the axoneme (A9) and is no longer present with UNC-GFP at the basal body apposed to the nuclei at the spermatid heads (A10). (A4–10) Nuclei are labeled with Hoechst. (A1 and 6) Early G2 spermatocytes. (A2 and 7) Late G2 spermatocytes. (A3 and 8) Round spermatids. (A4, 5, 9, and 10) Elongating spermatids. (B) CBY-TOMATO expression is similar in *Rfx*⁺/⁺ and *Rfx*⁻/⁻ spermatocytes and spermatids. Centrioles are labeled with γ-tubulin antibody. Bars, 5 μm.
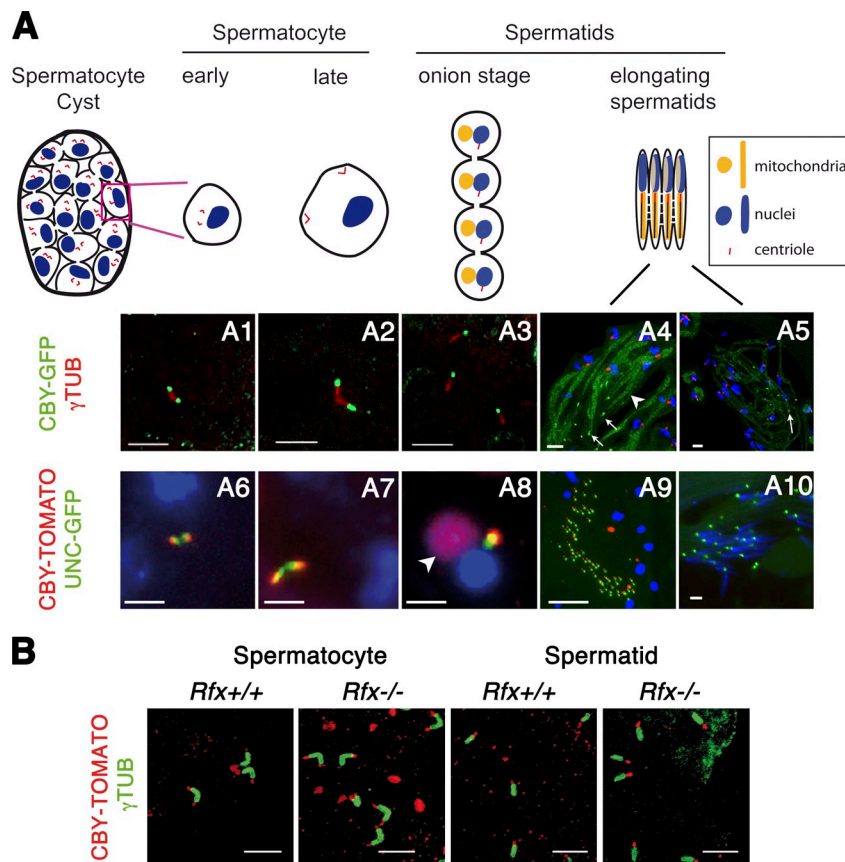
centrioles in dividing spermatogonia before the spermatocyte stage (unpublished data). In contrast to sensory neurons, *cby* expression in the testis does not require RFX (Fig. 3 B), consistent with RFX expression in spermatids only after the onset of *cby* expression (Vandaele et al., 2001).

During spermatid elongation, CBY was not maintained at the basal body but was observed at the tip of the growing axoneme until late spermatid differentiation (Fig. 3, A4, 5, 9, and 10). CBY was also found transiently associated with the mitochondria in onion-stage spermatids and early elongating spermatids (white arrowheads in Fig. 3, A8 and A4).

UNC is also located at both the basal body and growing tip of the axoneme (Baker et al., 2004; Wei et al., 2008). We observed that CBY-Tomato and UNC-GFP appeared together at the tip of the elongating centrioles in early G2 spermatocytes and remained there during spermatocyte maturation to spermatids, as the centrioles converted to basal bodies, with CBY localized in a zone that overlaps and extends more distal to UNC (Fig. 3, A6–8). However, during axoneme elongation, when CBY and UNC were both found at the tip of the growing axoneme, only UNC was maintained at the basal body (Fig. 3, A9 and 10).

Our observations show that CBY is localized at the distal end of maturing basal bodies in *Drosophila*. Interestingly, this localization is conserved in mammals in which CBY was found at the tip of the basal body of primary cilia in inner medullary collecting duct 3 (IMCD3) cells and above basal bodies of motile cilia in primary ependymal cells (Fig. S3).

cby is required for normal behavior, mechanosensation, and male fertility but not for Wg signaling

To understand the precise function of CBY, we constructed a null mutation, *cby¹*, using homologous recombination (Maggert et al., 2008) to delete most of the *cby* coding region (Fig. 4 A). PCR performed with primers designed on Fig. 4 A show that recombination occurred correctly on the left and right arms of the construct and that *cby* sequences are deleted in the *cby¹* allele (Fig. S1). In addition, we sequenced the entire recombinant region and confirmed that coding sequences of exon 2 are removed without affecting the adjacent genes.

RT-PCR on mRNA extracted from *cby¹/¹* flies detected no *cby* mRNA (Fig. S1), whereas expression of the two adjacent genes was not affected. In addition, *cby¹/¹* homozygotes and heterozygotes for *cby¹* and *Df(3R)BSC805*, a complete deficiency of the region, showed similar survival, overall behavior, and fertility (see the following three paragraphs; Figs. 4 and S1), confirming that *cby¹* is a null allele.

Homozygous *cby¹/¹* and *cby¹/Df(3R)BSC805* mutants were viable, but their behavior was altered, and males appeared to be hypofertile (Figs. 4 and S1). Wild-type flies show negative geotaxis; they move upward on vertical surfaces. This can be assayed with a simple climb test in which the percentages of flies that climb to different heights in a tube are measured after tapping them to the bottom. Whereas most control flies reached and stayed at the top of the tube in the first minute, most *cby¹/¹* or *cby¹/Df(3R)BSC805* flies stayed at the bottom of the tube
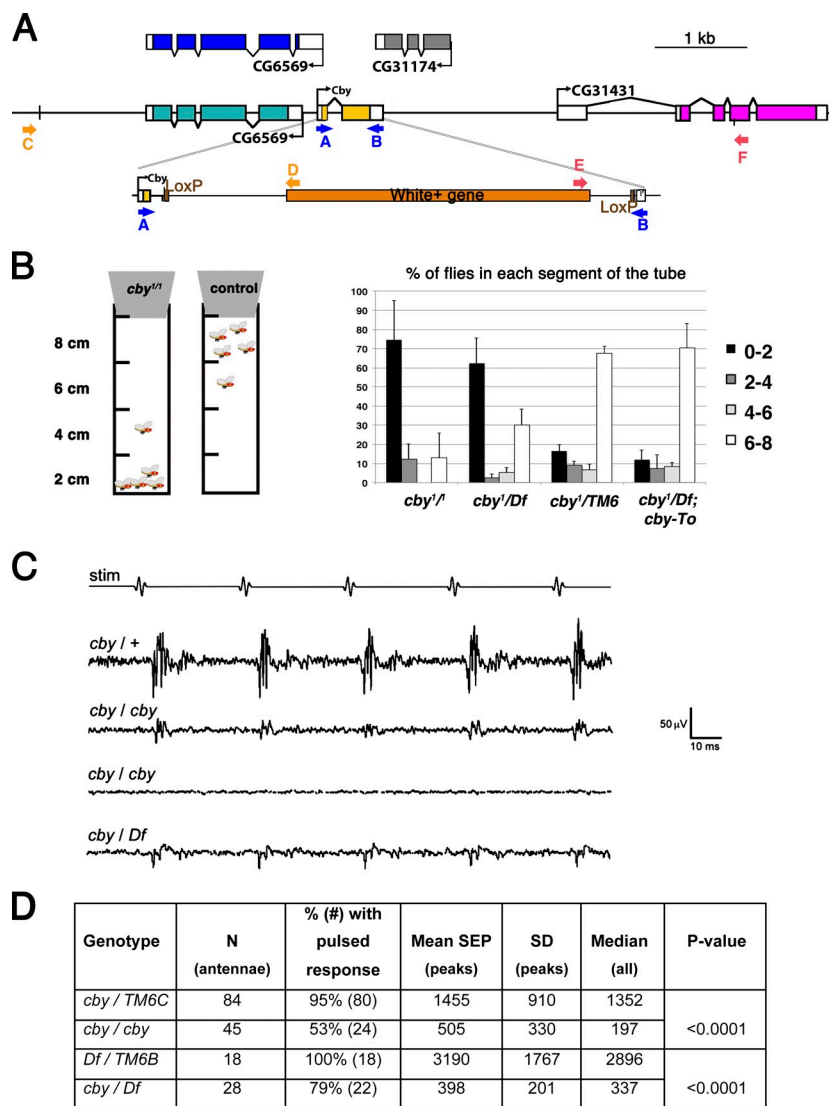
Figure 4. **Inactivation of *cby* leads to defective behavior and mechanosensation.** (A) Diagram of the *cby* genomic locus. The second coding exon was replaced by homologous recombination with a miniwhite gene flanked by two LoxP sites. The primers designed to screen for the recombinant events are indicated in yellow for the left arm and red for the right arm. (B) Diagram representing the bang assay to evaluate fly coordination. The number of flies that reach a defined level in the tube is counted 1 min after tapping the tube. *cby^{1/1}* flies and *cby^1/Df(3R)BSC805 (cby^1/Df)* stay at the bottom of the tube compared with control flies. The phenotype is rescued by adding one copy of the *cby-Tomato* transgene. *n* = 30 flies per assay. Error bars represent the SD of five assays. (C) Antennal nerve potentials recorded from age-matched sib *cby/TM6C* heterozygotes (*cby/+*), *cby* homozygotes (*cby/cby*), and from *Df(3R)BSC805/TM6B (Df/TM6B)* and *cby/Df(3R)BSC805 (cby/Df)* sibs in response to a five-pulse sound stimulus (stim). Each trace represents the averaged responses to 10 stimuli. Traces shown are those closest to the mean values for their respective genotypes. The third trace is representative of mutant recordings that do not show discernible SEP peaks. (D) Summary of sound-evoked nerve potential amplitudes. Mean and median peak amplitudes of the antennal SEPs for each indicated genotype. Mean values are derived only from those recordings showing discernible peaks; medians are from all recordings.

Genotype	N (antennae)	% (#) with pulsed response	Mean SEP (peaks)	SD (peaks)	Median (all)	P-value
cby / TM6C	84	95% (80)	1455	910	1352	
cby / cby	45	53% (24)	505	330	197	<0.0001
Df / TM6B	18	100% (18)	3190	1767	2896	
cby / Df	28	79% (22)	398	201	337	<0.0001

(Fig. 4 B). This phenotype was rescued by one copy of the CBY-Tomato transgene, confirming that CBY is required for negative geotaxis.

This change in geotaxis behavior could be a result either of a defect in gravity perception or locomotor coordination or both. Gravity is mainly sensed in *Drosophila* by antennal chordotonal organs (COs; Kamikouchi et al., 2009; Sun et al., 2009), whereas general locomotor coordination relies principally on external mechanosensory organs, with some contributions by COs. The *cby^{1/1}* behavioral phenotype was milder than the one observed in *atonal* mutants, which lack all COs (Jarman et al., 1993), or in transient receptor potential vanilloid channel or *tilB* mutants, which lack CO function (Eberl et al., 2000; Kavlie et al., 2010), and was much less severe than the extreme uncoordination seen in flies that lack mechanotransduction in bristles (Kernan et al., 1994) or lack all cilia (*Sas-4* or *Rfx* mutant flies; Dubruille et al., 2002; Basto et al., 2006). This indicates that mechanosensation is not completely abolished in *cby^{1/1}* flies.

We confirmed a defect in mechanosensation by recording antennal sound-evoked potentials (SEPs), which depend on mechanotransduction in the antennal CO (Eberl et al., 2000; Eberl and

Boekhoff-Falk, 2007). For each antenna, we measured the maximum amplitude of the averaged responses to 10 standard stimuli that mimic the pulse phase of courtship song. The antennal response amplitude in *cby^{1/1}* and in *cby^1/Df(3R)BSC805* was strongly reduced compared with controls (Fig. 4 C). Further, whereas 95% of the control antennae showed a pulsatile response, many of the *cby^{1/1}* and *cby^1/Df(3R)BSC805* antennae lacked any response. These observations lead us to conclude that *cby^1* mutants are partially defective in chordotonal-mediated mechanotransduction.

Because CBY was initially described as a negative regulator of Wg signaling in *Drosophila* (Takemaru et al., 2003), we carefully checked *cby^{1/1}* flies for phenotypes associated with loss or gain of Wg signaling. We did not observe any expansion of *engrailed* expression domains (*n* = 21) nor any cuticular defects (*n* = 119) in offspring embryos from homozygous *cby^{1/1}* male and female parents, which lack any parental or zygotic contributions (Fig. S2). Because Wg gain-of-function signaling leads to characteristic bristle phenotypes on the wing and the notum (Treisman et al., 1997), we also looked carefully at bristle number and distribution in *cby^{1/1}* adult flies (*n* = 31) but found no significant alterations (Fig. S2 D). Together, these

Figure 5. Ultrastructural defects of the chordotonal cilia in *cby*-deficient flies. (top left) Scheme and longitudinal section of a typical leg or antennal CO composed of two neurons ensheathed by a scolopale cell and linked to the cap cell at the tip of the ciliary endings. The cilia are anchored on a distal basal body (DBB) aligned above the proximal basal body (PBB) at the end of the dendrite. (a1–5) Sections at the level of the ciliary axoneme. In control legs (a1), axonemes are composed of nine peripheral microtubule doublets. (a2–5) *cby*[1/1] axonemes show a reduced number of microtubule doublets (a2 and 3), altered symmetry (a4), or extra microtubules (a5). (b1–3) Sections at the distal TZ. (b1) In control samples, a dense ring structure of ninefold symmetry is observed. (b2 and 3) In *cby*[1/1] antennae, interrupted, incomplete, and misformed ring structures are observed. (c1–3) Sections at the proximal TZ level. (c1) In control TZ, decorations connecting the membrane can be seen and likely correspond the Y links. (c2 and 3) In *cby*[1/1] antennae, decoration are interrupted (black arrows; c2), or the ninefold symmetry of the TZ decorations is interrupted (c3). (d1–3) Sections at the level of the proximal basal body. Bars, 0.5 µm. (d1) Basal bodies are anchored to the cell membrane by dense fibers in control flies (black arrow). Tight junctions connect the two dendrites. (d2 and 3) Two examples showing missing basal bodies in *cby*[1/1] flies. (e1–3) Longitudinal sections of *cby*[1/1] ciliary endings. In several cases (e1 and 2), the TZ is discontinuous (white arrows). (e2 and 3) Membrane bulges are observed along the cilia (black arrows). (f1–3) Low magnifications of transverse sections of scolopidia. Bars, 0.5 µm. (f1) Two axonemes are present in control antenna. (f2 and 3) Only one or no axoneme is sometimes observed in *cby*[1/1] antennae.
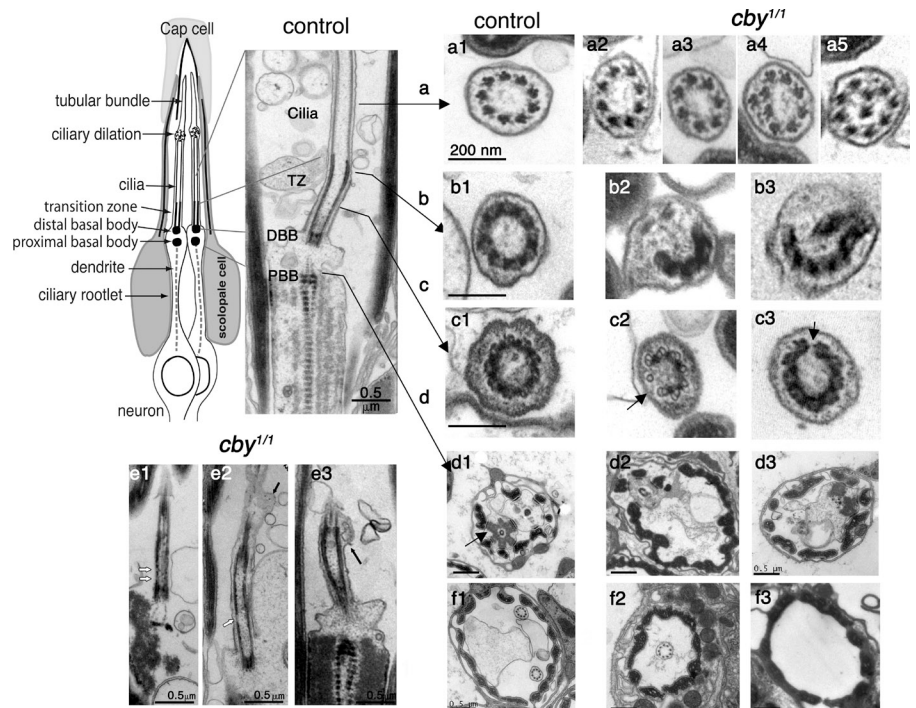
observations demonstrate that *Drosophila* CBY is needed for basal body–associated functions but not to mediate or regulate Wg signaling.

CBY is required for axonemal integrity and protein trafficking into and out of sensory neuronal cilia

For a detailed understanding of the role of CBY in basal bodies, we examined ciliary ultrastructure in *cby*[1/1] flies and controls. CO units or scolopidia are composed of two or three neurons that each extends a cilium from the tip of their sensory process (Fig. 5, top left). EM of COs in adult fly legs or antenna showed that cilia were missing in 26% of the mutant scolopidia (Fig. 5, f2 and 3). When ciliary profiles were present, we observed characteristic ultrastructural defects that were never seen in controls. The most frequent defect was a reduced number of microtubule doublets (19%; Fig. 5, a2 and 3). In rare cases (1%), extra doublets were observed, or the symmetry of the axoneme was abnormal (Fig. 5, a4 and 5). The remaining 80% of *cby*[1/1] chordotonal cilia were ultrastructurally normal, which is in agreement with the relatively mild behavioral defects observed in *cby*[1/1] flies. We also investigated the TZ and basal body region in *cby*[1/1] flies. The two basal bodies in each chordotonal neuron are aligned along their center axes, one distal to the other (Fig. 5). However, basal bodies are embedded in electron-dense material, and individual microtubules cannot be visualized by EM. In control flies, all basal bodies of chordotonal neurons appear as doughnut-shaped profiles with fibers connecting the basal body to the dendritic membrane (Fig. 5, d1). In *cby*[1/1] mutant flies, some of the basal body structures were completely missing

(22%; Fig. 5, d2 and 3). At the level of the TZ, which we believe to correspond to the Y link region (Fig. 5, cross-sections b and c), we could observe either completely interrupted symmetry (Fig. 5, b2 and 3) or more subtle discontinuities in the microtubule-associated structures of the TZ (black arrows in Fig. 5, c2 and 3). Discontinuities in the TZ could also be observed on longitudinal sections (white arrows in Fig. 5, e1 and 2) in addition to membrane bulges (black arrows in Fig. 5, e2 and 3) that were never observed in controls. Together, these results show that *cby* is required for correct axoneme assembly in *Drosophila* and that its absence leads to improper TZ formation. As we never observed missing basal bodies by γ-tubulin staining of ciliated neurons (unpublished data), the EM observations also suggest that basal bodies, though present in all neurons, are not positioned properly at the base of the cilia in some neurons.

Because ultrastructural defects were incompletely penetrant in *cby*[1/1] flies, we hypothesized that *cby* has a more subtle role in cilia biogenesis, as described for TZ proteins in other organisms (Ishikawa and Marshall, 2011). In *C. elegans*, TZ-associated proteins play an important role in admitting specific proteins into the cilia (Williams et al., 2011). Thus, we looked at the distribution of proteins known to traffic into the cilia. The first, NOMPB, is an IFT component (IFT88/Polaris) required for anterograde transport into the cilia (Han et al., 2003). We observed that NOMPB strongly accumulated in *cby*[1/1] embryonic cilia compared with discontinuous accumulation of NOMPB in control cilia (Fig. 6, A and B). Conversely, CG11356, the *Drosophila* ortholog of Arl13b, which couples anterograde and retrograde IFT (Caspary et al., 2007; Li et al., 2010b),
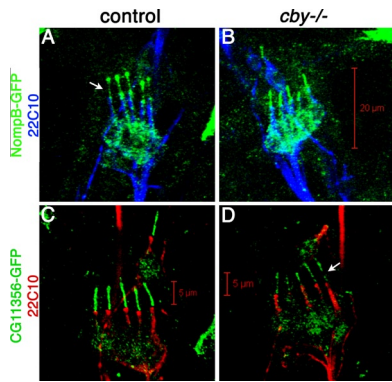
Figure 6. **CBY is required for IFT protein distribution.** (A–D) Expression of NompB/IFT88 (A and B) and CG11356/ARL13b (C and D) in either control (A and C) or $cby^{1/1}$ embryonic chordotonal cilia (B and D). (A and B) NompB-GFP accumulation is increased in $cby^{1/1}$ cilia compared with control cilia (white arrow). (C and D) CG11356-GFP accumulates continuously in control cilia, but its accumulation is punctuated in $cby^{1/1}$ cilia (white arrow). The overall abundance of CG11356 is also reduced in mutant cilia.

showed reduced accumulation in $cby^{1/1}$ cilia compared with controls (Fig. 6, C and D). These results show that ciliary-directed protein trafficking is altered in $cby^{1/1}$ flies.

CBY is required for basal body maturation in *Drosophila* spermatogenesis

$cby^{1/1}$ males are hypofertile (Fig. S1), and CBY is associated with the maturing basal body during spermatogenesis (Fig. 3). To understand its function during spermatogenesis, we looked at the structure of mutant sperm cysts. Differential interference contrast microscopy of live squashes of *Drosophila* testis showed no cellular defects in spermatocyte-stage cysts; all were composed of 16 cells showing that *cby* is not needed for spermatogonial divisions ($n = 12$; unpublished data).

When cysts in $cby^{1/1}$ testes were examined by EM, we frequently observed (88%) a reduced number of spermatids in each mature cyst. Each set of 16 spermatocytes should give rise to 64 spermatids, and all control cyst sections do show 63–64 spermatid profiles (Fig. 7 A). An altered number of spermatids was sometimes seen in early spermatid cysts, suggesting a possible meiotic defect (four out of six $cby^{1/1}$ cysts had 62 or fewer spermatids, whereas five out of five control cysts had 63–64 cells; Fig. 7 B). But no significant variations were seen in the ratio of nuclei-to-mitochondrial (Nebenkern) derivatives in onion-stage cysts, even though some aberrant spermatids could sometimes be observed (two or three aberrant cells in 3 out of 14 cysts; unpublished data). Hence, meiosis defects do not seem to be prevalent in $cby^{1/1}$ testis.

In early $cby^{1/1}$ spermatid sections, mitochondrial derivatives with no axoneme could be observed (2%; $n = 294$; Fig. 7 B, white arrow) as well as axonemes with no visible mitochondria derivatives (3.4%; $n = 294$; Fig. 7 B, arrowhead), which were never observed in controls. We also observed partially penetrant (14%; $n = 294$) but reproducible defects of the axonemal ultrastructure. Incomplete axonemal structures were found (white arrows in Fig. 7, C and D) with a reduced number of microtubule doublets. Because these defects were visible in early spermatids, we hypothesize that CBY is required for normal axoneme assembly.
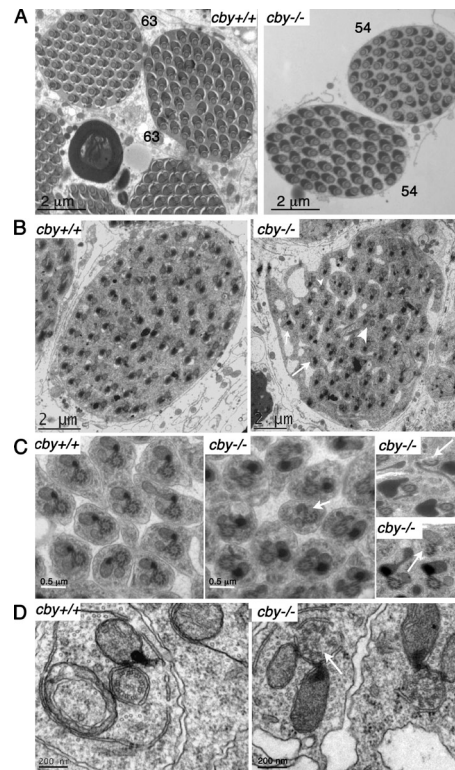
Figure 7. **CBY is required for axonemal organization in the testis.** (A) $cby^{1/1}$ mutant testes still produce mature spermatozoids, but their number is reduced. The spermatid cysts are disorganized, and the number of spermatid per cysts is often compromised. (B) Young spermatid cysts are disorganized and contain a reduced number of spermatids. Some axonemes are not associated with mitochondrial derivatives (white arrowhead), and some mitochondrial derivatives are not associated with an axoneme (white arrow). (C) In addition, a few axonemes are misorganized in mutant flies (white arrows) with mainly missing doublets. Bars, 0.5 µm. (D) High magnification of young spermatids highlighting the ultrastructural defects that can be observed on growing axonemes (white arrow). Bars, 200 nm.

Altogether, our observations indicate that CBY plays an important function during spermatid differentiation in *Drosophila*.

Because UNC is a basal body–associated protein that is also required for axonemal assembly in *Drosophila*, we looked at UNC distribution in *cby* mutant testis. Remarkably, we observed that UNC deposition during spermatocyte maturation was severely affected, with UNC being deposited on a longer and more variable length of the elongating centrioles compared with controls (Fig. 8, A and B). The paired elongating centrioles in $cby^{1/1}$ testes often showed unequal extents of UNC protein (Fig. 8 B, white arrow) in contrast to the symmetrical UNC deposition in the controls. This aberrant UNC distribution is maintained in early spermatids (Fig. 8, C, D [white arrows], E, and F). Later, during spermatid differentiation, UNC labeling at the basal body was reduced in $cby^{1/1}$ testis compared with controls (Fig. 8, G and H). In contrast, no differences were observed between *cby* mutants and controls in γ-tubulin labeling (unpublished data). Hence, altered UNC deposition could either reflect a direct action of CBY on UNC deposition or indirectly reflect a more general basal body formation defect. Altogether, these results show that CBY is required for proper centriole-to–basal body conversion in *Drosophila* spermatocytes.

control   *cby¹ᐟ¹*

UNC-GFP γ-TUB

UNC-GFP DNA / Transmitted light

Spermatocytes | Early spermatids | Early spermatids | Spermatids
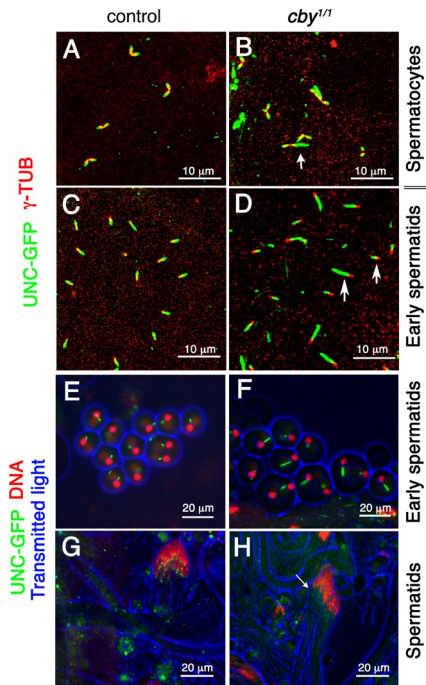
Figure 8. UNC distribution associated with basal body function is altered in *cby¹ᐟ¹* testis. (A–H) Distribution of UNC-GFP and γ-tubulin (γ-TUB) was observed by antibody staining in fixed testis from control (A and C) or *cby¹ᐟ¹* (B and D) flies or by GFP fluorescence in live squashed preparations of control (E and G) or *cby¹ᐟ¹* testis (F and H). (A and B) The extent of UNC protein deposition is irregular in *cby¹ᐟ¹* spermatocytes compared with control. The two apposed centrioles stained for γ-tubulin show equivalent UNC labeling in control but not in *cby¹ᐟ¹* spermatocytes (white arrow). (C–F) UNC labeling marks an increased length segment in *cby¹ᐟ¹* early spermatids (white arrows). (G and H) In *cby¹ᐟ¹* elongating spermatids, UNC staining at the basal body is diffuse and not limited to a dot, as shown in controls. Some faint UNC staining, not observed in controls, is also observed along the axoneme. The arrow points to the reduced and diffuse UNC staining at the base of the nucleus in *cby* mutant testis. (E–H) DNA stained with DAPI.

Discussion

We show that *cby* plays an important function in the two *Drosophila* cell types in which centrioles mature to basal bodies. In sensory cilia, CBY is required for proper TZ assembly and modulates protein trafficking into or out of the cilium. In the testis, we observed that CBY is required for centriole conversion to a basal body and for proper completion of spermatogenesis. In conclusion, our work demonstrates that CBY has an ancestral function in basal body biogenesis. Notably, we find no evidence for a CBY function in Wg signaling in *Drosophila*.

CBY is a novel component of the sensory cilium TZ

CBY is associated with the TZ in cilia. The TZ is a molecularly and ultrastructurally distinct axoneme domain located just distal to the basal body. The ultrastructure of the TZ differs between primary cilia and motile cilia and also between species (for a comprehensive review, see Fisch and Dupuis-Williams [2011]). Nevertheless, several components of the TZ are conserved in many ciliated organisms. Several groups of TZ proteins are associated with human diseases, such as nephronophthisis (NPHP),

MKS, and Joubert syndrome (Hodges et al., 2010). TZ proteins can be grouped in functional modules by their pattern of cooccurrence across species and because mutations in each group cause similar sets of symptoms in humans. The MKS functional module is conserved in most of the ciliated organisms, but the NPHP module is not found in all species and in particular not in *Drosophila* (Hodges et al., 2010). We show here that CBY is a novel component of the TZ, which colocalizes with CG14870 (B9D1/MKSR1), a component of the MKS module (Bialas et al., 2009). CBY is found in animals with motile cilia but not in *C. elegans*, suggesting a specific function in TZs of motile cilia in animals. In agreement with this hypothesis, *cby* mutant mice show defects in biogenesis of motile cilia as a result of defective docking of the basal bodies at the apical membrane (Voronina et al., 2009). However, in *Drosophila*, CBY is found at the tip of the basal bodies, both in cells with motile cilia or flagella (chordotonal neurons and spermatids) and also in neurons that innervate external sensory (ES) organs such as bristles. ES cilia lack the canonical axonemal cytoskeleton, and dynein arms are tightly ensheathed by a surrounding matrix and, so, are unlikely to be motile. We do not know whether CBY has any function in ES cells. No behavioral defects were seen when *cby* mutant larvae were challenged with chemical or olfactory stimuli (unpublished data), nor did mutant adults show the severe uncoordination that characterizes bristle loss-of-function mutations, suggesting that CBY is not essential for the function of ES cilia. CBY may be more essential in motile CO cilia than in ES organs. Or, the moderate structural defects in *cby* mutant axonemes may be more consequential for the function of motile cilia than for static ES cilia. Perhaps, as for the MKS module proteins in nematode sensory cilia (Williams, et al., 2011), ES phenotypes may become evident when other TZ proteins are also mutated.

In mouse, a ciliary requirement for CBY may also be limited to motile cilia because *cby*-deficient embryos, unlike mutants with complete ciliogenesis defects, survive until birth and mostly show defects in airway motile ciliogenesis. However, we observed that CBY was localized at the TZ of primary cilia in IMCD3 cells (Fig. S1), suggesting a more general function of CBY at the TZ. A function for CBY in primary cilia could explain the observation that *cby* mutant mice show defects in lung development that are thought to result from WNT signaling defects (Love et al., 2010). In agreement with a function for CBY in primary cilia, injection of a truncated dominant form of CBY in LLC-PK1 cells reduces the number of cells with primary cilia (Hoffmeister et al., 2011).

CBY is required for protein trafficking into or out IFT-dependent cilia

Several TZ proteins have been shown to be required for protein trafficking into the cilia and for IFT-dependent processes. This has clearly been demonstrated for NPHP1, NPHP4, and NPHP6 in *C. elegans* for several of the MKS-associated proteins and for NPHP1 in mammalian photoreceptors (Jauregui et al., 2008; Jiang et al., 2009; Williams et al., 2011). We show here that at least two proteins involved in IFT are abnormally distributed in *cby¹ᐟ¹* chordotonal cilia, NOMPB/IFT88 accumulating in cilia

to higher levels than normal, and Arl13 being depleted. This could either result from an altered balance between anterograde and retrograde IFT transport or from altered gating of proteins into the cilia. We do not know precisely all the TZ structures that are affected in $cby^{1/1}$ cilia, but we observe some defects at the level of what likely corresponds to the Y-linker region of the TZ also called champagne glass structures (Fisch and Dupuis-Williams, 2011). In *C. elegans*, mutants lacking MKS/MKSR/NPHP proteins show missing connecting links, suggesting that these proteins are either associated with components of the connecting Y links or are required for their stability (Williams et al., 2011). In addition, nematodes with defects in MKSR1 and NPHP4 show ultrastructural defects of the cilia, such as a reduction in the number of microtubule doublets, that are similar to the defects observed in $cby^{1/1}$ flies (Williams et al., 2011). Altogether, these observations suggest that CBY plays a function at the TZ similar to the one of MKS and NPHP complexes. MKS proteins belonging to the B9 domain family (MKS1, B9D1, and B9D2) are conserved in *Drosophila*, but most of the NPHP proteins are not. Conversely, CBY is not found in *C. elegans*, where most of the NPHP proteins are conserved. Hence, these different modules likely operate independently. Such variations in the architecture and function of the TZ between organisms still need to be understood.

CBY and UNC, another TZ protein in *Drosophila*, show similar phenotypes

Only few other proteins associated with the TZ in *Drosophila* have been functionally analyzed. Among them, UNC is also a coiled-coil–containing protein but is found in only Dipteran species, where it diverged rapidly. It has also been suggested that UNC could be functionally equivalent to human OFD1, a centrosomal and basal body coiled-coil protein mutated in the ciliopathy oro-facial-digital syndrome 1 (Baker et al., 2004). We observed that loss of CBY function affects UNC protein accumulation during centriole-to–basal body conversion in spermatocyte. This could reflect an altered basal body structure in $cby^{1/1}$ testes but could also reflect that UNC and CBY functionally interact during TZ assembly. In support of this latter hypothesis, the basal bodies in $unc^{-/-}$-deficient sensory neurons show defects similar to *cby* mutant flies with broken basal body/TZ rings, missing cilia, or disrupted cilia (Baker et al., 2004). $unc^{-/-}$ flagella also have incomplete axonemes like in $cby^{1/1}$ testis. Thus, UNC and CBY could work together in a functional module required for centriole maturation in *Drosophila* testis. The $unc^{-/-}$ phenotype is more penetrant than the $cby^{1/1}$ phenotype, suggesting that *unc* is more limiting than *cby* for basal body/TZ assembly.

Interestingly, a novel protein, DILATORY (DILA), was identified recently as interacting with UNC in *Drosophila* chordotonal neurons (Ma and Jarman, 2011). This suggests that CBY, UNC, and DILA may function together at the TZ. However, in chordotonal neurons of *dilatory* mutants, ultrastructural defects were restricted to the cilia but did not apparently affect the TZ. Moreover, no flagellar axonemal defects are associated with *dila* mutations (Ma and Jarman, 2011), suggesting that CBY acts differently from *dila* in basal body function. Investigating the genetic and biochemical interactions between *cby* and *dila* will help dissect the pathway by which basal bodies mature in *Drosophila* and in other animals in which both *cby* and *dila* are conserved.

Function of the TZ and primary cilium-like extension in *Drosophila* spermatocytes

We observed that CBY, like UNC and DILA, is deposited at the tip of the maturing centriole in *Drosophila* spermatocytes. The maturing centrioles are associated with cytoplasmic vesicles before reaching the plasma membrane (Tates, 1971; unpublished data), where they grow small cilium-like extensions. Altogether, these observations suggest that a structure molecularly similar to the TZ assembles during centriole maturation in *Drosophila* spermatocytes and is maintained during meiosis and spermatid elongation. Indeed, both UNC and CBY are found to be associated with the tip of the growing axoneme, suggesting that this TZ-like structure is maintained during flagellar assembly. TZ assembly does not require IFT (Williams et al., 2011), which is consistent with the observations that IFT is not required for *Drosophila* spermatogenesis (Han et al., 2003; Sarpal et al., 2003). Therefore, we propose that the primary cilium-like structure assembled in *Drosophila* spermatocytes more likely corresponds to an elongated TZ from the maturing centriole, which hence behaves like a basal body. Therefore, we hypothesize that flagellar growth in *Drosophila* is similar to TZ assembly, which would explain also why flagella assembly is IFT independent in *Drosophila*.

Interestingly, in UNC-deficient spermatocytes, the primary cilia/TZs are shorter, showing that UNC is involved in elongating these primary cilia/TZ (Baker et al., 2004). Whereas primary cilia-like extensions were easily observed in wild-type testis, we did not observe any centrioles that were anchored to the plasma membrane in $cby^{1/1}$ flies. We also did not manage to observe enough centrioles to describe precisely their distal ultrastructure. However, because UNC deposition is severely affected in $cby^{1/1}$ spermatocytes, CBY appears to be required to control either directly or indirectly the assembly of the TZ in these cells.

The function of the spermatocyte primary cilia is unknown. Centrioles are dispensable for postembryonic development in *Drosophila* (Basto et al., 2006) but are required for male meiosis, as observed in *sas-4* or *sak/plk4*-deficient flies (Rodrigues-Martins et al., 2008; Riparbelli and Callaini, 2011), even though spermatids can still form without axonemes (Bettencourt-Dias et al., 2005; Basto et al., 2006). BLD10 is required in *Drosophila* both for centriole elongation spermatocytes and to complete meiosis, suggesting a possible meiotic requirement for centriole elongation (Mottier-Pavie and Megraw, 2009; Carvalho-Santos et al., 2010). However, no precise description of the primary cilia ultrastructure in spermatocytes has been described in *Bld10* mutants. Among the other proteins that are required for basal body biogenesis in *Drosophila* (Gogendeau and Basto, 2010), only UNC is associated with specific defects in spermatocyte primary cilia. Therefore, it will be interesting to examine in more detail primary cilia assembly in mutants for other TZ proteins and to finely examine meiosis and early spermatid differentiation defects.

The reduced number of early spermatids in cysts and aberrant mitochondrial derivative numbers suggest that *cby* might play a role in meiosis. We know that this phenotype is not a result of improper centriole distribution, as γ-tubulin staining showed that all spermatocytes and spermatids had the right number of centrioles. Our results could also implicate CBY in early spermatid survival or in elongation, which would lead to a reduced number of spermatid profiles in some cyst sections. In *Drosophila*, spermatid elongation relies on microtubule-dependent mitochondria remodeling (Noguchi et al., 2011). CBY is transiently associated with mitochondria in onion-stage and early elongating spermatids. Spermatids do elongate in *cby^1/1* flies, but we do not know whether elongation is as complete as in control testis. The function of CBY in mitochondria during spermatid elongation needs to be more thoroughly investigated.

CBY and WNT signaling

In mammals, CBY has at least two functions. Analysis of *cby^−/−* mice demonstrates that *cby* is required for basal body anchoring during multiciliated cell differentiation, illustrating that *cby* has conserved this anchoring function throughout evolution. Experiments in cell cultures indicate that CBY is involved in WNT signaling in different cell types, essentially by controlling nuclear–cytoplasmic shuttling of β-catenin, the WNT signaling pathway effector (Takemaru et al., 2003, 2009; Li et al., 2007, 2008, 2010a; Singh et al., 2007; Mokhtarzada et al., 2011). CBY directly interacts with β-catenin, and WNT signaling defects have been described during lung development of *cby* knockout mice (Love et al., 2010). A previous RNAi-based study suggested that *cby* could also be involved in Wg signaling in *Drosophila* (Takemaru et al., 2003). However, Wg signaling and development appear normal in *cby^1/1*-null flies, ruling out a function of *cby* in Wg signaling in *Drosophila*. Off-target RNAi effects may have caused the observed defects in the previous study. We do not know whether CBY interacts with β-catenin in *Drosophila*, but, if so, such an interaction would have consequences only in the ciliated cells in which *cby* is expressed.

Therefore, we conclude that CBY function in WNT signaling has either been acquired during chordate evolution or lost in the Dipteran lineage. In mammals, CBY interacts with cis-Golgi–associated proteins and is implicated in polycystin-2 distribution in cilia, even though this capacity remains controversial (Hidaka et al., 2004; Hoffmeister et al., 2011). A function in vesicular transport from the Golgi is consistent with CBY function in TZ assembly, which starts when centrioles fuse to vesicular membranes likely derived from the Golgi apparatus inside the cytosol. CBY could be required early for basal body–to-membrane attachment and also for vesicular trafficking to the cilia. Whereas CBY is not found associated with most of the cis-Golgi apparatus in cultured mammalian cells, a small pool of the cis-Golgi protein GMAP210 localizes next to CBY at the base of motile cilia (Fig. S3). This is compatible with a possible function in cis-Golgi vesicular trafficking to the cilia, as demonstrated for polycystin-2 transport (Hoffmeister et al., 2011).

Conclusions

Together, our data demonstrate that CBY is required for the assembly of the ciliary TZ in *Drosophila* both in sensory neurons and in male germ cells.

Materials and methods

cby coding sequence

Comparison of *cby* cDNA and genomic sequences in different *Drosophila* strains showed a consistent insertion of two base pairs in the 3′ end of the *cby* coding sequence compared with the gene annotation on the FlyBase database. The consequence of this insertion (in italics) is a slight change in the C-terminal protein sequence starting at amino acid 121. Five amino acids are different (italic) and are followed by eight additional amino acids at the C terminus: 5′-*CAT*GCGACGGAACTAAGTGAGCTGAAGCCA-AAGGAAAAGTGA-3′ (*H A T E L* S E L K P K E K *).

BLAST and sequence alignment

BLAST searches used as a query the *cby* gene sequence from FlyBase, modified as described in the previous section, using the basic local alignment search tool from the National Center for Biotechnology Information. The sequences obtained were then aligned using SeaView software.

Reporter constructs

All primer sequences are described in Table S1.

CBY-GFP. A 1,350-bp fragment including *cby* coding sequences and upstream regulatory sequences was amplified by PCR from wild-type *Drosophila* genomic DNA using the following primers designed from the noncorrected *cby* sequence: Cby-pro5 and Cby-pro3/BamHI. The resulting PCR fragment was cloned into the EcoRI and BamHI sites of the pW8-GFP plasmid (Loppin et al., 2005), in frame with the *Gfp* sequence.

CBY-Tomato. The *Tomato* sequence was obtained by PCR on the Zeo-TomatoNT-2 (a gift from R. Basto, Institut Curie, Paris, France) with the introduction of an AgeI site at the 5′ end and a STOP and NotI site at the 3′ end. The resulting PCR fragment was cloned in the BglII and NotI sites of the pattB plasmid. The complete *cby* 3′ untranslated region (UTR) was cloned downstream of the *Tomato* sequence in the pattB-Tomato plasmid obtained above using XhoI and XbaI restriction sites introduced in the 3′ UTR PCR fragment.

cby coding and upstream regulatory sequences (1,375 bp) were amplified using the Cby-pro5 forward primer and a Cby-PRO3/AgeI reverse primer based on the corrected *cby* sequence with the addition of an AgeI site at the 3′ end. The resulting PCR product was cloned in the EcoRI and AgeI sites of the pattB-Tomato-3′cbyUTR plasmid in frame with the *Tomato* sequence. Transgenic lines were established by P element–mediated germline transformation (Spradling, 1986) or by phiC31-mediated germline transformation for the pattB plasmid–derived constructs (Bischof et al., 2007).

CG14870-6xMycTag reporter. A 2,942-bp fragment covering *CG14870* coding and upstream regulatory sequences was amplified by PCR on wild-type *Drosophila* genomic DNA with primers F-14870/BamHI and R-14870/NotI. The resulting PCR product was cloned in frame with the 6xMycTag in the modified pattB plasmid containing the 6xMycTag and SV40polyA sequences. Transgenic lines were obtained from BestGene Inc.

pW8-GFP CG11356. A 4,230-bp fragment covering *CG11356* coding sequences and upstream regulatory sequences was amplified by PCR on wild-type *Drosophila* genomic DNA with the primers CG 11356-PRO3 and CG 11356-PRO5. The resulting PCR fragment was cloned into the pW8-*Gfp* plasmid. Transgenic lines were obtained by P element transformation.

cby homologous recombination

The *cby* gene was disrupted by ends-out homologous recombination (Maggert et al., 2008). The left and right arms of the targeting construct were amplified by PCR on genomic DNA of the y[1] w[*]; P{ry[+t7.2] = 70FLP}11 P{v[+t1.8] = 70I-SceI}2B noc[Sco]/CyO, S[2] stock using primers F-3′cby/SphI, R-3′cby/NotI, F-5′cby/BsiWI, and R-5′cby/AscI. The resulting construct enabled the deletion of most of exon 2, including the stop codon, and the acceptor splice site of intron 1 (Fig. 4 A). All the coding regions from the cloned 5′ and 3′ homologous fragment were verified by sequencing. Transgenic lines were established by phiC31-mediated germline transformation (Bischof et al., 2007) and used for homologous recombination, as previously described (Maggert et al., 2008).

Fly stocks

We thank J. Schmitt and P. Morales (both from Centre de Génétique et de Physiologie Moléculaire et Cellulaire, Université Claude Bernard Lyon 1,

Villeurbanne, France) for *Drosophila* medium and stock maintenance. The chromosomes and alleles P{unc-GFP}[34a], nompB[1], and P{GFP:nompB} were previously described (Han et al., 2003; Baker et al., 2004). P{unc-GFP}[34a] is inserted on the second chromosome and encodes the entire UNC protein fused to GFP in the C terminus. nompB[1] is a loss-of-function allele of nompB that deletes 1,100 bp of exon 3 and part of exon 4. P{GFP:nompB} is inserted on the third chromosome and encodes the full-length NOMPB protein fused to GFP at its N terminus. {Ubq55:RFP:sas4} was a gift from R. Basto. Df(3R)BSC805 was obtained from the Bloomington Stock Center and uncovers the 93F13-94A6 cytological interval. All the other following fly strains were constructed in the laboratory: w; P{cby::GFP}[F23]/CyO; P{cby::GFP}[M27], w; P{cby::GFP}[F23]/CyO; rfx[253] e/TM3, P{GAL4-twi.G}[2.3], P{UAS-2xEGFP}[AH2.3], w; P{cby::GFP}[F23]/CyO; rfx[49]/TM3, P{GAL4-twi.G}[2.3], P{UAS-2xEGFP}[AH2.3], w; Bl/CyO; P{cby::Tomato}attP62E1[M1F2]/TM6B, w; P{cby::Tomato}attP62E1 rfx[253] e/TM6B, st rfx[16] e ca/TM6B Tb Dr, w; cby[1]/TM3, P{GAL4-twi.G}[2.3], P{UAS-2xEGFP}[AH2.3], w; P{cby::GFP}[F23]/CyO; cby[1]/TM6B, w; P{cby::GFP}[F23]/CyO;P{cby::GFP}[M27] cby[1]/TM6B, w;P{unc-GFP}[34a]/CyO;P{cby::Tomato}attP62E1[M1F2]/TM6B, w; P{unc-GFP}[34a]/CyO; cby[1]/TM3, P{GAL4-twi.G}[2.3], P{UAS-2xEGFP}[AH2.3], y w P{CG11356::GFP}[F6M1]/FM7, w, w; P{GFP::nompB} cby[1]/TM3, P{GAL4-twi.G}[2.3], P{UAS 2xEGFP}[AH2.3], w; P{CG14870-myc}attP59D3/CyO; cby[1]/TM3, P{GAL4-twi.G}[2.3], P{UAS 2xEGFP}[AH2.3], and w; P{CG14870-myc}attP59D3/CyO; P{cby::Tomato}attP62E1[M1F2]/TM6B.

SEPs
Extracellular compound potentials were recorded with tungsten electrodes placed in the antenna and head, as previously described (Eberl et al., 2000; Eberl and Kernan, 2011). Each fly was mounted in a micropipette tip and its proboscis fixed in wax so that its antennae were exposed and free to move. A computer-generated sound stimulus (five pulses of a 500-Hz sine wave at 35-ms intervals) was amplified by an audio amplifier (Realistic MPA-30; RadioShack) and an 8-in, 4-Ω speaker and brought to the fly via 0.25-in Tygon tubing, with its opening placed close enough to the antennae to ensure near-field sound conditions. To record antennal nerve potentials, one electrolytically sharpened tungsten wire electrode was placed between the first and second antennal segments and a second in the head. The differential alternating current signal from these was amplified (5,000× gain) by a BMA-200 Bioamplifier (CWE, Incorporated) and digitized and analyzed using an Instrunet 100B A/D converter and SuperScope II software (GW Instruments, Inc). The same stimulus amplitude was used for all recordings. Flies were chilled briefly at 0°C for mounting. Flies that were sorted under CO_2 anesthesia were allowed to recover for >40 h before recording. Mutant (cby[1/1] or cby[1]/Df) flies were recorded alternately with their age-matched control sibs. For each antenna, we measured the maximum amplitude of the averaged responses to 10 sound stimuli. P-values were calculated from the Mann–Whitney rank sum test, with all responses lacking peaks tied at the lowest rank.

Bang assay
The climbing test was performed on female flies of the same age. 30 flies were placed in graduated tubes and banged on the table at t = 0. Pictures were taken every minute for 5 min and analyzed by counting the number of flies present in each interval every minute and for each genotype.

Live squashes of testes
Late pupae were dissected once in PBS 1×. The dissected testes were transferred on a slide in a drop of PBS 1× containing 8.3 mg/ml Hoechst 33342 and then squashed under a coverslip before being observed live using a microscope (Imager Z1; Carl Zeiss).

Immunostaining
Precisely staged embryos were sorted and collected in PBS 1×/0.1% Triton X-100 and dechorionated in bleach. Embryos were rinsed in PBS 1×, extracted from the vitelline membrane using a tungsten needle, transferred to a polylysine-coated slide, and dissected. Embryos were fixed in 4% PFA/PBS 1× (20 min), rinsed, and blocked in PBT (PBS 1×, 5% BSA, and 0.1% Triton X-100). Embryos were incubated with primary antibodies diluted in PBT washed in PbT (PBS 1×, 0.1% BSA, and 0.1% Triton X-100) and incubated with secondary antibodies diluted in PbT. Embryos were washed in PTW (0.1% Tween 20 in PBS 1×) and mounted (Cytomation; Dako).

Whole-mount testis preparation was performed as follows: testes were fixed 15 min in 4% PFA/PBS 1× followed by a 15-min treatment in PBS 1× and 0.1% Triton X-100, blocked in 1% BSA in PBS 1×, and incubated with primary antibodies overnight at 4°C. Testes were incubated

with secondary antibodies for 2 h at room temperature. Testis squashes were performed as follows: testis (0–2-d adults) were fixed 20 min at room temperature in 3.7% PFA/PBS 1× and flattened under a coverslip on a microscope slide pretreated with 10% polylysine solution. Slides were quick frozen in liquid nitrogen, and coverslips were removed, fixed in chilled 95% ethanol for 5 min, washed twice in PBT (PBS 1× containing 0.1% Triton X-100), and blocked for at least 1 h in PBTB (PBT with 3% BSA) at room temperature. Samples were incubated overnight at 4°C with primary antibodies diluted in PBTB and 2 h at room temperature in secondary antibodies in PBTB. Testes were mounted in mounting medium (Cytomation).

The antibodies used are as follows: rabbit anti-GFP (1:500; Invitrogen), anti-HRP (1:3,000; Jackson ImmunoResearch Laboratories, Inc.), anti-ASL (1:500; provided by R. Basto), anti-DPLP (1:1,000; provided by R. Basto), anti–γ-tubulin (used on embryos; 1:400; Sigma-Aldrich), mouse monoclonal anti-GFP (1:1,000; Roche), anti-22C10 (1:250; provided by S. Benzer, California Institute of Technology, Pasadena, CA), anti-myc (1:3,000; Euromedex), and anti–γ-tubulin (used on testes; 1:100; Sigma-Aldrich). The secondary antibodies used, diluted at 1:1,000, are as follows: goat anti–mouse Alexa Fluor 488 conjugated, 546 conjugated, and 647 conjugated; goat anti–rabbit Alexa Fluor 488 and 555 conjugated (Invitrogen); and goat anti–rabbit Cy5 conjugated (GE Healthcare).

Image acquisition
Slides were analyzed at room temperature on a microscope (Imager Z1) equipped with 20× Plan-NEOFLUAR (0.5 NA) and 40× Plan-NEOFLUAR (0.75 NA) objectives or a 63× Plan-NEOFLUAR (NA 1.25) objective. Epifluorescence images were acquired with a charge-coupled device camera (CoolSNAP HQ2, Roper Scientific) and MetaView software (Molecular Devices). Confocal stacks were acquired with a confocal microscope (LSM 510 META; Carl Zeiss) and software equipped with 63× Plan-Apochromat (1.4 NA), 40× Plan-NEOFLUAR (1.3 NA), and 25× Plan-NEOFLUAR (0.8 NA) objectives. Image brightness and contrast were adjusted by using ImageJ (National Institutes of Health), and separate panels were assembled with Photoshop software (CS4; Adobe). Capture times and adjustments were identical for compared images on one figure. γ was set to 1 in all figure panels.

EM
Antennae, legs, and testes were dissected in PBS 1× and fixed in 2% glutaraldehyde, 0.5% PFA, and 0.1 M Na-cacodylate, pH 7.4, for 48 h at 4°C. After three washes of 15 min in 0.15 M sodium cacodylate, pH 7.4, samples were postfixed in 1% OsO_4 for 4 h for antennae and 1 h for testes. Samples were then dehydrated through ethanol series and propylene oxide and embedded in Epon medium (Fluka). Ultrathin sections were cut on an ultramicrotome (Leica). Sections were contrasted in Ultrastainer (Leica) in aqueous uranyl acetate and lead citrate. Contrasted sections were observed on a transmission electron microscope (CM120; Philips). Images were acquired with a 2k × 2k digital camera (ORIUS 200; Gatan) and digital micrograph software. Images were processed with Photoshop software (CS4). Only contrast and brightness were adjusted.

Cell cultures
Mouse primary ependymal cell cultures were derived from mouse newborn brains (OF1 strain), as previously described (El Zein et al., 2009). IMCD3 cell lines (a gift from P. Goggolidou, Mammalian Genetics Unit, Medical Research Council, Harwell, Oxfordshire, England, UK) were cultured in DME/F12 medium containing 10% FBS, 100 U/ml penicillin, 100 µg/ml streptomycin, and 1× nonessential amino acids (reagents from GE Healthcare). Ependymal and IMCD3 cells were seeded on polylysine- and laminin-coated glass coverslips. Confluent ependymal cells were fixed the day of serum deprivation or after 12 d of serum deprivation, whereas IMCD3 cells were fixed after 2 d of culture in 0.5% FBS containing medium. Cells were fixed in methanol for 5 min at −20°C or in 4% PFA for 15 min at room temperature when using the anti-Arl13b primary antibody. After permeabilization in 0.1% Triton X-100 for 10 min, cells were blocked 2 h in 5% FBS in PBS 1× followed by an overnight primary antibody incubation using the following: mouse anti-Cby antibody (1:200; Santa Cruz Biotechnology, Inc.), rabbit anti-Arl13b (1:500; a gift from T. Caspary, Emory University, Atlanta, GA), rabbit anti–γ-tubulin (1:100; Sigma-Aldrich), and rabbit anti-GMAP210 (1:4,000; a gift from M. Bornens, Institut Curie, Paris, France). Immunostaining was revealed with goat anti–mouse Alexa Fluor 488 and goat anti–rabbit Alexa Fluor 555–conjugated antibodies (1:500; Invitrogen). The slides were mounted in the presence of DAPI or DRAQ5 in fluorescence mounting medium (Dako). Slides were visualized under a microscope (AxioImager Z1; Carl Zeiss) and a confocal microscope (LSM 510 META).

RT-PCR

Total RNA of w^{1118} and $cby^{1/1}$ testes was extracted using TRIZOL (Invitrogen) and treated with DNase (Invitrogen). cDNA was obtained using 1 µg of DNase-treated RNA, 200 ng of random primers (Promega), and 200 U of RevertAid H Minus M-MuLV reverse transcription (Thermo Fisher Scientific) in a final volume of 30 µl. 1 µl cDNA was used for PCR reactions.

Online supplemental materials

Fig. S1 shows the molecular characterization of the cby^1 allele and quantification of $cby^{1/1}$ male fertility. Fig. S2 shows the absence of any Wg-associated phenotype in cby^1 flies. Fig. S3 shows the distribution of mouse CBY protein in IMCD3 or ependymal cells. Table S1 lists all primers used for creating reporter constructs and the cby^1 allele. Online supplemental material is available at http://www.jcb.org/cgi/content/full/jcb.201109148/DC1.

References

Ajima, R., and H. Hamada. 2011. Wnt signalling escapes to cilia. *Nat. Cell Biol.* 13:636–637. http://dx.doi.org/10.1038/ncb0611-636

Avidor-Reiss, T., A.M. Maer, E. Koundakjian, A. Polyanovsky, T. Keil, S. Subramaniam, and C.S. Zuker. 2004. Decoding cilia function: Defining specialized genes required for compartmentalized cilia biogenesis. *Cell.* 117:527–539. http://dx.doi.org/10.1016/S0092-8674(04)00412-X

Baker, J.D., S. Adhikarakunnathu, and M.J. Kernan. 2004. Mechanosensory-defective, male-sterile unc mutants identify a novel basal body protein required for ciliogenesis in *Drosophila*. *Development.* 131:3411–3422. http://dx.doi.org/10.1242/dev.01229

Basto, R., J. Lau, T. Vinogradova, A. Gardiol, C.G. Woods, A. Khodjakov, and J.W. Raff. 2006. Flies without centrioles. *Cell.* 125:1375–1386. http://dx.doi.org/10.1016/j.cell.2006.05.025

Bettencourt-Dias, M., A. Rodrigues-Martins, L. Carpenter, M. Riparbelli, L. Lehmann, M.K. Gatt, N. Carmo, F. Balloux, G. Callaini, and D.M. Glover. 2005. SAK/PLK4 is required for centriole duplication and flagella development. *Curr. Biol.* 15:2199–2207. http://dx.doi.org/10.1016/j.cub.2005.11.042

Bialas, N.J., P.N. Inglis, C. Li, J.F. Robinson, J.D. Parker, M.P. Healey, E.E. Davis, C.D. Inglis, T. Toivonen, D.C. Cottell, et al. 2009. Functional interactions between the ciliopathy-associated Meckel syndrome 1 (MKS1) protein and two novel MKS1-related (MKSR) proteins. *J. Cell Sci.* 122:611–624. http://dx.doi.org/10.1242/jcs.028621

Bischof, J., R.K. Maeda, M. Hediger, F. Karch, and K. Basler. 2007. An optimized transgenesis system for *Drosophila* using germ-line-specific phiC31 integrases. *Proc. Natl. Acad. Sci. USA.* 104:3312–3317. http://dx.doi.org/10.1073/pnas.0611511104

Briggs, L.J., J.A. Davidge, B. Wickstead, M.L. Ginger, and K. Gull. 2004. More than one way to build a flagellum: Comparative genomics of parasitic protozoa. *Curr. Biol.* 14:R611–R612. http://dx.doi.org/10.1016/j.cub.2004.07.041

Carvalho-Santos, Z., P. Machado, P. Branco, F. Tavares-Cadete, A. Rodrigues-Martins, J.B. Pereira-Leal, and M. Bettencourt-Dias. 2010. Stepwise evolution of the centriole-assembly pathway. *J. Cell Sci.* 123:1414–1426. http://dx.doi.org/10.1242/jcs.064931

Caspary, T., C.E. Larkins, and K.V. Anderson. 2007. The graded response to Sonic Hedgehog depends on cilia architecture. *Dev. Cell.* 12:767–778. http://dx.doi.org/10.1016/j.devcel.2007.03.004

Dubruille, R., A. Laurençon, C. Vandaele, E. Shishido, M. Coulon-Bublex, P. Swoboda, P. Couble, M. Kernan, and B. Durand. 2002. *Drosophila* regulatory factor X is necessary for ciliated sensory neuron differentiation. *Development.* 129:5487–5498. http://dx.doi.org/10.1242/dev.00148

Eberl, D.F., and G. Boekhoff-Falk. 2007. Development of Johnston's organ in *Drosophila*. *Int. J. Dev. Biol.* 51:679–687. http://dx.doi.org/10.1387/ijdb.072364de

Eberl, D.F., and M.J. Kernan. 2011. Recording sound-evoked potentials from the *Drosophila* antennal nerve. *Cold Spring Harb. Protoc.* 2011:prot5576. http://dx.doi.org/10.1101/pdb.prot5576

Eberl, D.F., R.W. Hardy, and M.J. Kernan. 2000. Genetically similar transduction mechanisms for touch and hearing in *Drosophila*. *J. Neurosci.* 20:5981–5988.

El Zein, L., A. Ait-Lounis, L. Morlé, J. Thomas, B. Chhin, N. Spassky, W. Reith, and B. Durand. 2009. RFX3 governs growth and beating efficiency of motile cilia in mouse and controls the expression of genes involved in human ciliopathies. *J. Cell Sci.* 122:3180–3189. http://dx.doi.org/10.1242/jcs.048348

Fisch, C., and P. Dupuis-Williams. 2011. Ultrastructure of cilia and flagella - back to the future! *Biol. Cell.* 103:249–270. http://dx.doi.org/10.1042/BC20100139

Fuller, M.T. 1993. Spermatogenesis. *In* The Development of Drosophila melanogaster. Vol. 1. M. Bate and A.M. Arias, editors. Cold Spring Harbor Laboratory Press, Cold Spring Harbor, NY. 71–147.

Goetz, S.C., and K.V. Anderson. 2010. The primary cilium: A signalling centre during vertebrate development. *Nat. Rev. Genet.* 11:331–344. http://dx.doi.org/10.1038/nrg2774

Gogendeau, D., and R. Basto. 2010. Centrioles in flies: The exception to the rule? *Semin. Cell Dev. Biol.* 21:163–173. http://dx.doi.org/10.1016/j.semcdb.2009.07.001

Hampl, V., L. Hug, J.W. Leigh, J.B. Dacks, B.F. Lang, A.G. Simpson, and A.J. Roger. 2009. Phylogenomic analyses support the monophyly of Excavata and resolve relationships among eukaryotic "supergroups". *Proc. Natl. Acad. Sci. USA.* 106:3859–3864. http://dx.doi.org/10.1073/pnas.0807880106

Han, Y.G., B.H. Kwok, and M.J. Kernan. 2003. Intraflagellar transport is required in *Drosophila* to differentiate sensory cilia but not sperm. *Curr. Biol.* 13:1679–1686. http://dx.doi.org/10.1016/j.cub.2003.08.034

Hidaka, S., V. Könecke, L. Osten, and R. Witzgall. 2004. PIGEA-14, a novel coiled-coil protein affecting the intracellular distribution of polycystin-2. *J. Biol. Chem.* 279:35009–35016. http://dx.doi.org/10.1074/jbc.M314206200

Hodges, M.E., N. Scheumann, B. Wickstead, J.A. Langdale, and K. Gull. 2010. Reconstructing the evolutionary history of the centriole from protein components. *J. Cell Sci.* 123:1407–1413. http://dx.doi.org/10.1242/jcs.064873

Hoffmeister, H., K. Babinger, S. Gürster, A. Cedzich, C. Meese, K. Schadendorf, L. Osten, U. de Vries, A. Rascle, and R. Witzgall. 2011. Polycystin-2 takes different routes to the somatic and ciliary plasma membrane. *J. Cell Biol.* 192:631–645. http://dx.doi.org/10.1083/jcb.201007050

Hoyer-Fender, S. 2010. Centriole maturation and transformation to basal body. *Semin. Cell Dev. Biol.* 21:142–147. http://dx.doi.org/10.1016/j.semcdb.2009.07.002

Ishikawa, H., and W.F. Marshall. 2011. Ciliogenesis: Building the cell's antenna. *Nat. Rev. Mol. Cell Biol.* 12:222–234. http://dx.doi.org/10.1038/nrm3085

Jarman, A.P., Y. Grau, L.Y. Jan, and Y.N. Jan. 1993. atonal is a proneural gene that directs chordotonal organ formation in the *Drosophila* peripheral nervous system. *Cell.* 73:1307–1321. http://dx.doi.org/10.1016/0092-8674(93)90358-W

Jauregui, A.R., K.C. Nguyen, D.H. Hall, and M.M. Barr. 2008. The *Caenorhabditis elegans* nephrocystins act as global modifiers of cilium structure. *J. Cell Biol.* 180:973–988. http://dx.doi.org/10.1083/jcb.200707090

Jiang, S.T., Y.Y. Chiou, E. Wang, Y.L. Chien, H.H. Ho, F.J. Tsai, C.Y. Lin, S.P. Tsai, and H. Li. 2009. Essential role of nephrocystin in photoreceptor intraflagellar transport in mouse. *Hum. Mol. Genet.* 18:1566–1577. http://dx.doi.org/10.1093/hmg/ddp068

Kamikouchi, A., H.K. Inagaki, T. Effertz, O. Hendrich, A. Fiala, M.C. Göpfert, and K. Ito. 2009. The neural basis of *Drosophila* gravity-sensing and hearing. *Nature.* 458:165–171. http://dx.doi.org/10.1038/nature07810

Kavlie, R.G., M.J. Kernan, and D.F. Eberl. 2010. Hearing in *Drosophila* requires TilB, a conserved protein associated with ciliary motility. *Genetics.* 185:177–188. http://dx.doi.org/10.1534/genetics.110.114009

Kernan, M., D. Cowan, and C. Zuker. 1994. Genetic dissection of mechanosensory transduction: Mechanoreception-defective mutations of *Drosophila*. *Neuron.* 12:1195–1206. http://dx.doi.org/10.1016/0896-6273(94)90437-5

King, N., M.J. Westbrook, S.L. Young, A. Kuo, M. Abedin, J. Chapman, S. Fairclough, U. Hellsten, Y. Isogai, I. Letunic, et al. 2008. The genome of the choanoflagellate *Monosiga brevicollis* and the origin of metazoans. *Nature.* 451:783–788. http://dx.doi.org/10.1038/nature06617

Laurençon, A., R. Dubruille, E. Efimenko, G. Grenier, R. Bissett, E. Cortier, V. Rolland, P. Swoboda, and B. Durand. 2007. Identification of

novel regulatory factor X (RFX) target genes by comparative genomics in *Drosophila* species. *Genome Biol.* 8:R195. http://dx.doi.org/10.1186/gb-2007-8-9-r195

Li, F.Q., A.M. Singh, A. Mofunanya, D. Love, N. Terada, R.T. Moon, and K. Takemaru. 2007. Chibby promotes adipocyte differentiation through inhibition of beta-catenin signaling. *Mol. Cell. Biol.* 27:4347–4354. http://dx.doi.org/10.1128/MCB.01640-06

Li, F.Q., A. Mofunanya, K. Harris, and K. Takemaru. 2008. Chibby cooperates with 14-3-3 to regulate β-catenin subcellular distribution and signaling activity. *J. Cell Biol.* 181:1141–1154. http://dx.doi.org/10.1083/jcb.200709091

Li, F.Q., A. Mofunanya, V. Fischer, J. Hall, and K. Takemaru. 2010a. Nuclear-cytoplasmic shuttling of Chibby controls beta-catenin signaling. *Mol. Biol. Cell.* 21:311–322. http://dx.doi.org/10.1091/mbc.E09-05-0437

Li, Y., Q. Wei, Y. Zhang, K. Ling, and J. Hu. 2010b. The small GTPases ARL-13 and ARL-3 coordinate intraflagellar transport and ciliogenesis. *J. Cell Biol.* 189:1039–1051. http://dx.doi.org/10.1083/jcb.200912001

Loppin, B., E. Bonnefoy, C. Anselme, A. Laurençon, T.L. Karr, and P. Couble. 2005. The histone H3.3 chaperone HIRA is essential for chromatin assembly in the male pronucleus. *Nature*. 437:1386–1390. http://dx.doi.org/10.1038/nature04059

Love, D., F.Q. Li, M.C. Burke, B. Cyge, M. Ohmitsu, J. Cabello, J.E. Larson, S.L. Brody, J.C. Cohen, and K. Takemaru. 2010. Altered lung morphogenesis, epithelial cell differentiation and mechanics in mice deficient in the Wnt/β-catenin antagonist Chibby. *PLoS ONE*. 5:e13600. http://dx.doi.org/10.1371/journal.pone.0013600

Ma, L., and A.P. Jarman. 2011. Dilatory is a *Drosophila* protein related to AZI1 (CEP131) that is located at the ciliary base and required for cilium formation. *J. Cell Sci.* 124:2622–2630. http://dx.doi.org/10.1242/jcs.084798

Maggert, K.A., W.J. Gong, and K.G. Golic. 2008. Methods for homologous recombination in *Drosophila*. *Methods Mol. Biol.* 420:155–174. http://dx.doi.org/10.1007/978-1-59745-583-1_9

Mokhtarzada, S., C. Yu, A. Brickenden, and W.Y. Choy. 2011. Structural characterization of partially disordered human Chibby: Insights into its function in the Wnt-signaling pathway. *Biochemistry*. 50:715–726. http://dx.doi.org/10.1021/bi101236z

Mottier-Pavie, V., and T.L. Megraw. 2009. *Drosophila* bld10 is a centriolar protein that regulates centriole, basal body, and motile cilium assembly. *Mol. Biol. Cell.* 20:2605–2614. http://dx.doi.org/10.1091/mbc.E08-11-1115

Noguchi, T., M. Koizumi, and S. Hayashi. 2011. Sustained elongation of sperm tail promoted by local remodeling of giant mitochondria in *Drosophila*. *Curr. Biol.* 21:805–814. http://dx.doi.org/10.1016/j.cub.2011.04.016

Riparbelli, M.G., and G. Callaini. 2011. Male gametogenesis without centrioles. *Dev. Biol.* 349:427–439. http://dx.doi.org/10.1016/j.ydbio.2010.10.021

Rodrigues-Martins, A., M. Riparbelli, G. Callaini, D.M. Glover, and M. Bettencourt-Dias. 2008. From centriole biogenesis to cellular function: Centrioles are essential for cell division at critical developmental stages. *Cell Cycle*. 7:11–16. http://dx.doi.org/10.4161/cc.7.1.5226

Rosenbaum, J.L., and G.B. Witman. 2002. Intraflagellar transport. *Nat. Rev. Mol. Cell Biol.* 3:813–825. http://dx.doi.org/10.1038/nrm952

Sarpal, R., S.V. Todi, E. Sivan-Loukianova, S. Shirolikar, N. Subramanian, E.C. Raff, J.W. Erickson, K. Ray, and D.F. Eberl. 2003. *Drosophila* KAP interacts with the kinesin II motor subunit KLP64D to assemble chordotonal sensory cilia, but not sperm tails. *Curr. Biol.* 13:1687–1696. http://dx.doi.org/10.1016/j.cub.2003.09.025

Singh, A.M., F.Q. Li, T. Hamazaki, H. Kasahara, K. Takemaru, and N. Terada. 2007. Chibby, an antagonist of the Wnt/beta-catenin pathway, facilitates cardiomyocyte differentiation of murine embryonic stem cells. *Circulation*. 115:617–626. http://dx.doi.org/10.1161/CIRCULATIONAHA.106.642298

Sorokin, S.P. 1968. Centriole formation and ciliogenesis. *Aspen Emphysema Conf.* 11:213–216.

Spradling, A.C. 1986. P element-mediated transformation. *In Drosophila*: A Practical Approach. D. Roberts, editor. IRL Press, Oxford, England, UK. 175–189.

Sun, Y., L. Liu, Y. Ben-Shahar, J.S. Jacobs, D.F. Eberl, and M.J. Welsh. 2009. TRPA channels distinguish gravity sensing from hearing in Johnston's organ. *Proc. Natl. Acad. Sci. USA*. 106:13606–13611. http://dx.doi.org/10.1073/pnas.0906377106

Takemaru, K., S. Yamaguchi, Y.S. Lee, Y. Zhang, R.W. Carthew, and R.T. Moon. 2003. Chibby, a nuclear beta-catenin-associated antagonist of the Wnt/Wingless pathway. *Nature*. 422:905–909. http://dx.doi.org/10.1038/nature01570

Takemaru, K., V. Fischer, and F.Q. Li. 2009. Fine-tuning of nuclear-catenin by Chibby and 14-3-3. *Cell Cycle*. 8:210–213. http://dx.doi.org/10.4161/cc.8.2.7394

Tates, A.D. 1971. Cytodifferentiation during spermatogenesis in *Drosophila melanogaster*. PhD thesis. J.H. Pasmans, The Hague, Netherlands. 162 pp.

Treisman, J.E., A. Luk, G.M. Rubin, and U. Heberlein. 1997. eyelid antagonizes wingless signaling during *Drosophila* development and has homology to the Bright family of DNA-binding proteins. *Genes Dev.* 11:1949–1962. http://dx.doi.org/10.1101/gad.11.15.1949

Vandaele, C., M. Coulon-Bublex, P. Couble, and B. Durand. 2001. *Drosophila* regulatory factor X is an embryonic type I sensory neuron marker also expressed in spermatids and in the brain of *Drosophila*. *Mech. Dev.* 103:159–162. http://dx.doi.org/10.1016/S0925-4773(01)00340-9

Voronina, V.A., K. Takemaru, P. Treuting, D. Love, B.R. Grubb, A.M. Hajjar, A. Adams, F.Q. Li, and R.T. Moon. 2009. Inactivation of Chibby affects function of motile airway cilia. *J. Cell Biol.* 185:225–233. http://dx.doi.org/10.1083/jcb.200809144

Wallingford, J.B., and B. Mitchell. 2011. Strange as it may seem: The many links between Wnt signaling, planar cell polarity, and cilia. *Genes Dev.* 25:201–213. http://dx.doi.org/10.1101/gad.2008011

Wei, H.C., J. Rollins, L. Fabian, M. Hayes, G. Polevoy, C. Bazinet, and J.A. Brill. 2008. Depletion of plasma membrane PtdIns(4,5)P2 reveals essential roles for phosphoinositides in flagellar biogenesis. *J. Cell Sci.* 121:1076–1084. http://dx.doi.org/10.1242/jcs.024927

Williams, C.L., C. Li, K. Kida, P.N. Inglis, S. Mohan, L. Semenec, N.J. Bialas, R.M. Stupay, N. Chen, O.E. Blacque, et al. 2011. MKS and NPHP modules cooperate to establish basal body/transition zone membrane associations and ciliary gate function during ciliogenesis. *J. Cell Biol.* 192:1023–1041. http://dx.doi.org/10.1083/jcb.201012116